Tin-Bismuth Finishes and the Phenomenon of Whiskers

Sudarshan Lal & Thomas D. Moyer
FCI USA, Inc., Etters, Pennsylvania.

Abstract

Tin-lead coatings have been employed as preferred surface finishes on solder tails for the past five decades. The addition of lead in tin deposits has been shown to be beneficial in whisker mitigation. The use of other alloying elements such as copper, silver and bismuth has also been suggested in various lead-free surface finishes to mitigate whiskers. However, no single lead-free alloy combination has been universally implemented in all applications. The whiskering tendency has always been a major concern. Recently, interest has arisen in the use of tin-bismuth in separable connectors. This paper describes our studies on the process, the deposit characteristics, and the propensity of whisker formation under various conditions. Some practical applications along with their limitations shall be presented.

1. Introduction

The lead-free transition is picking up speed. Companies are feverishly working on qualification of their products for lead-free applications due to impending restrictions of hazardous substances (ROHS) such as lead, mercury, chromium and brominated flame retardants. The time for compliance is fast approaching. Strenuous efforts are being devoted to research and development to explore lead-free substitutes as tangible surface finishes. Several alternate lead-free finishes are being proposed and tested by commercial bath suppliers and end users. One of the simplest lead-free finishes is pure matte tin, although, it has a potential risk for tin whiskers [1]. Besides pure matte tin, use of binary alloys like tin-silver, tin-zinc, tin-bismuth and ternary alloys like Sn-Bi-Sb, has been also proposed. A literature survey [2-4] shows sparse studies on tin-bismuth system. Recently, interest has been generated in tin-bismuth plating due to continually improving bath chemistries. This paper describes our technical findings on a commercial tin-bismuth chemistry with respect to the process, deposit characteristics, stress levels and whiskering propensity. The limitation of tin-bismuth finishes in separable interfaces is also discussed.

2. Experimental Procedure

The tin-bismuth plating bath consists of five components; tin concentrate, bismuth concentrate, methane-sulfonic acid (MSA) concentrate as electrolyte, additives, and antioxidants. The bath was formulated as per guidelines provided by the bath supplier. Analysis of tin and acid was done by standard volumetric methods. Bismuth in the bath was monitored by atomic absorption spectroscopy (AA). The additive in the bath was monitored by UV-VIS spectroscopy. Bismuth in the deposit was determined by SEM-EDX analysis. This was also confirmed by dissolving the coating in aqua regia and measuring by AA.

Tin-bismuth plating was done on oxygen free high conductivity (OFHC) annealed copper foils with a 2 μm Ni under-layer. The plating studies were performed using a rotating shaft electrode (RSE) at 500 rpm in a 2L thermostated double walled pyrex beaker at 40 ºC. Tin anodes were used and plating deposited at current densities of 7.5 A/dm^2 (75 asf), and 15 A/dm^2 (150 asf) at 40ºC.

Total carbon in the deposit was determined by gas fusion technique by combusting a 1.5-2.0 gram sample. Adhesion test (ASTM B571-97), and coating thickness by X-ray spectrometry (ASTM B 568-98) were performed on plated foils.

Solderability on the plated foils was conducted as per ASTM method B678-86 (2001) using a meniscograph with a standard non-active flux under “as is” and after 8 hours of steam aging.

Macro-stress in films was determined using C-194 flexure beams and a commercial deposit stress analyzer. Thin (0.002 inch thick) metal strip pre-coated with resist on one side, was plated with a given film and deflection of the strip was noted at time t_0. Stresses were calculated by using simplified Stoney's equation [5] as shown below:

$$\sigma = E \quad T^2 \delta \quad / 3 L^2 t \text{ -------(1)}$$

Where σ is stress in deposit, Psi
E= Young's Modulus of Elasticity, 120,690
T= thickness of substrate in mm, 0.0520 mm
L= Length of plated area of one leg, 76.2 mm
δ = deflection from zero line, mm, ½ total spread in mm
t = thickness of deposit , mm

Residual stress and texture in plated films were studied by X-ray diffraction (XRD).

All samples were pre-conditioned by being subjected to 500 thermal shock (TS) cycles at temperatures ranging from –55 ºC to + 85 ºC with a 20 minute cycle, 10 minute dwell time. The plated foils, after thermal cycling, were exposed to two environmental conditions: a) room temperature and ambient humidity, labeled as "RT" and b) 55 ºC and 85% relative humidity, labeled as "HH". Whisker testing on "preconditioned" samples was performed according to iNEMI protocol [6] and examinations were conducted using scanning electron microscopy (SEM).
The impact of mechanical damage caused by scraping and compressive stress was studied on coupons and also on separable connectors with regard to their whisker response. In this case, actual product terminals were plated on a reel-to-reel set up.

3. Results

A- Sn-Bi Bath
1.1 Current Efficiency and Plating Rates

Current density effects on plating rates and respective current efficiencies (CE) at 20ºC are summarized in Table I. These experiments were done at room temperature for studying the plating rates and stress levels.

Table I
Effect of Current Density on Efficiency and Plating Rates

Current Density, A/dm^2	Plating Rate, µ"/sec	% Current Efficiency
7.5	2.39	94.2
15.0	3.89	91.3
22.5	4.78	58.4 *
30.0	0.34	7.4 *

* *Gassed profusely*

Bath efficiency is greater than 90% over a limited current density range of 7.5-15 A/dm^2 at room temperature. Beyond 22.5 A/dm^2, the current efficiency decreased dramatically. At higher current densities, the film appearance was darker, and copious evolution of hydrogen gas was observed. Gas evolution was one of the prominent reasons for decreased current efficiency. Since the bath should be operated at 40 ºC, a typical plot of C.D. vs. current efficiencies is presented in figure 2.

1.2 Temperature and Plating Rates

Effect of bath temperature on plating rates is shown in Table II. It is apparent that temperature has an insignificant effect on plating rates at varying current densities.

Table II

Temperature and Plating Rates (μ"/sec) at various Current Densities

CD, A/dm^2	Pl. Rate, 20º C	Pl. Rate, 30º C	Pl. Rate, 40º C
7.5	2.39	2.38	2.26
15.0	3.89	4.17	4.31
22.5	4.78	5.86	6.34
30.0	0.34	2.21	3.31

At all temperatures, plating rates decreased at 30 A/dm^2 due to side reactions especially copious evolution of hydrogen gas. Plating rates in current range (7.5-15 A/dm^2) were constant with decent current efficiencies. A current density > 25 A/dm^2 , a powdery deposit with reduced current efficiency was obtained. Figure 3 depicts a plot of c.d. versus plating rates showing highest plating rates at 25 A/dm^2.

3.3 Allowable Impurity levels in the bath

The stability of the plating bath may be affected due to the presence of impurities in the solution. Limits of certain impurities were established from general appearance of the coatings. For example Fe > 500 ppm was noted to cause turbidity in the bath. Similarly, copper contamination >50 ppm caused turbidity in the bath with poor deposit appearance. Chromium > 50 ppm was responsible for poor adhesion and increase in Ni > 200 ppm was responsible for poor solderability. The amount of lead in the bath should be < 20 ppm in order to fulfill the ROHS directive. Elevated levels of copper, iron and chromium tend to accelerate oxidation of Sn(II) to Sn (IV).

3.4 Agitation Effect

Effect of agitation (variation of rotation speed) on plating rates was studied and the relationship is shown in Figure 4. Plating rates tend to decrease with increasing rotation speed. These rates were at their maximum at 250 rpm and lowest at 1000 rpm. At a working range of 500-750 rpm, the plating rates were constant and appearance of deposits were acceptable.

3.5 Limitations in Sn-Bi Electrodeposition

The deposition of tin-bismuth is difficult due to the following factors:

i) Differences in standard electrode potentials (E_0) of tin and bismuth

Bi^{3+} + 3e -----------→ Bi^0 E_0 = +0.30V vs. SHE

Sn^{2+} + 2e --------- → Sn^0 E_0 = -0.14 V vs. SHE

A stable chelating system is required for co-deposition of bismuth and to ensure its deposit composition at varying current densities.

ii) Immersion plating of bismuth on tin anodes and substrates

$3Sn^0 + 4\ Bi^{3+}$ ----------→ $3\ Sn^{4+} + 4\ Bi^0$

iii) Oxidation of Sn(II) in presence of Bi(III)

$3Sn^{2+} + 2\ Bi^{3+}$ --------→ $3\ Sn^{4+} + 2\ Bi^0$

iv) Catalytic oxidation of Sn(II) in presence of air and metal impurities

$2Sn^{2+} + O_2 + 4\ H^+$ ---------→ $2\ Sn^{4+} + 2\ H_2O$

v) Reduced efficiency due to hydrogen evolution in acid electrolytes

$2\ H_3O^+ + e$ ----------→ $2\ H_2O + H_2$ (gas)

vi) Electrochemical degradation of additives and bismuth chelates
Additives play an important role in the electro-deposition process by grain refinement, leveling and brightening the deposits [7-8].
Decomposition of organics, and bismuth complexes results in formation of breakdown products causing deleterious effects on coatings with serious process implications, deposit properties and enhanced risk of whiskers.
We observed significant blackening of tin anodes due to immersion plating of bismuth. The bath developed a light tan color with rust type sediments on aging indicating its instability.

3.6 Effect of additive levels

Figure 5 depicts the effect of various levels of additives on plating rates. Higher amounts of additive had minimal effect on plating rates. Figure 6 shows the effect of additive concentration on current efficiencies. The CE is highest around 15.0 A/dm^2 and tends to decrease slightly (1.3%) in presence of highest concentration (60 ml/l) of the additive.

B- Tin Bismuth Deposit Characteristics

3.7 Appearance

The Sn-Bi coating was satiny matte in appearance when plated at current densities ranging from 7.5-15.0 A/dm^2. The finish was slightly darker on the edges at current density (cd) 22.5 A/dm^2, which was likely due to the higher effective current density at the edges. Some improvement in appearance was noticed at higher agitations. Coatings were powdery and dark gray in appearance at 30.0 A/dm^2 .

3.8 Adhesion

The standard tape test as per ASTM method B 571-97 indicated good adhesion with no peeling and cracking when bending the test coupons.

3.9Morphology and Grain Size

The morphology of Sn-Bi films plated at varying current densities using a standard bath are shown in Figure 1. Morphologies were similar in c.d. range (7.5-22.5 A/dm^2) up to a certain current density and changed significantly at 30 A/dm^2 . The deposit also became rough with coarse structure. Morphology and grain size appear to be influenced by current density and also deposit composition.

3.10 Total Carbon in Deposits

Copper foils plated with tin-bismuth (1.5-2.0 g) at 10 A/dm^2, and 15 A/dm^2 were subjected to gas fusion analysis. The total carbon found was 0.003 %. The carbon level was extremely low and did not pose any issues in dry bake, and solderability tests. The carbon levels did not seem to be current dependent and were significantly lower than the values for bright tin coatings, which usually have10-15 times higher carbon values. Low carbon in tin films implies that the stresses in the deposits are minimal. It is well known that whisker formation is accentuated in the presence of compressive internal stresses caused by co-deposited organic brighteners [9-11].

3.11 Solderability

Solderability was evaluated on a wetting balance by measuring the zero cross time (ZCT) which is the duration until buoyancy becomes zero due to wetting of the coating. Coverage >95% was achieved without any issues on samples "AS IS", and after 8 hours of steam aging. ZCT for Sn-Bi alloy was < 1 second. The wetting forces were similar to pure tin and Sn-Pb indicating acceptable solderability with good wetting.

3.12 Residual Stress and Texture

Residual stress and texture results (Table III) in the deposits obtained from solutions with two concentrations (3% & 10%) of bismuth were measured by Sin$^2\psi$ method using X-Rays diffraction technique [12].

Table III
Residual Stress and Texture Analysis

Sample	Stress, MPa	Pref. Orientation	Pref. Orientation
A	-11.7	<103> (77 %)	<112> (14 %)
B	-17.1	<103> (81%)	<112> (14%)

The residual stress determined by XRD was compressive in nature and the dominant preferred orientation was <103> in both samples irrespective of bismuth concentrations. The resolution limit for the method is +/-3.5 MPa. Macro-stress values obtained from flexure beams were tensile in nature with values around 1 MPa. The values tend to depend on film thickness. For example, at room temperature using CDA 194 copper stress values ranging from 0.4-2.0 MPa were recorded. These stress techniques have their limitations and sensitivity limits, which are responsible for differences in stress types and the values.

3.13 Whisker Results

a) Flat coupons
All plated films were "preconditioned" by subjecting to 500 thermal cycles. After TS, in absence of nickel underlayer, numerous protusions often called as odd shape eruptions (OSEs) were observed and their density increased with the film thickness (Fig.7-a,7-b). In presence of nickel, OSE density decreased singnificantly showing the effect of nickel barrier layer (Fig. 7-c). OSE density increased with increase in Sn-Bi film thickness even in the presence of Ni layer (Fig. 7-d). Essentially, these odd shape eruptions are the result of combination of stresses caused by oxidation of Sn-Bi film and thermal mismatch between the film and the under-layer substrate. In the presence of copper, stresses were caused due to chemical reaction of tin and copper forming IMC layer.
We noticed beneficial effect of bismuth in deposits with respect to whisker propensity. It appeared to retard formation of needle type tin whiskers. We did not come across any long needle shaped whisker except odd shape eruptions even after 6 months of exposures under both environments. We observed changes in microstructure with some corrosion under heat and high humidity (Figure 8).
Only small OSEs (5-10 µm) were observed and no needle type whiskers were found at room temperature and ambient humidity condition. With thicker films, OSEs density increased significantly under HH. No long whiskers with striations were observed over flat coupons.

b) Mechanical Stresses and Separable Interfaces

We have reported the whiskering behavior of various matte tin films on coupons and terminals extensively in our previous studies [13-15]. In assembled terminals, we observed long whiskers in mechanically damaged areas where the tin film was disturbed and scraped due to insertion of the terminal into plastic housings. Similarly, in the tin-bismuth finish, we observed formation of tin whiskers on mated terminals on a separable interface after 48 hours of mating with a continuous force. Whiskers tend to grow from the accumulated tin-bismuth coating, which was mechanically stressed, and had undergone plastic deformation during mating in a separable connector. We also noticed this phenomenon by subjecting a tin-bismuth film to 100 lbs of constant force for 96 hours. Tin whiskers were noticed at the periphery where the tin film was extruded due to mechanical impact. No bismuth in tin whisker was detected. In this case, whisker initiation may be due to the extraneous compressive stress on the coating. Our results are similar to Fisher et al. [16]. The compressive effects may be caused by mechanical factors or due to intrinsic stresses imposed in the coating due to formation of Sn-Cu intermetallics [17] by diffusion of copper in tin grain boundaries with the formation of Cu_6Sn_5 as shown by focused ion beam (FIB) cross-section (Figure 9).

Impact of Hertzian stress on separable interfaces was examined for whiskers formation on assembled connectors. A FFC male connector was mated with a FPC flex cable and preconditioned to TS. The whiskers were inspected at these interfaces after exposing to RT and HH conditions. The results are summarized in Table IV.

Table IV
Whiskers in microns at Separable Interfaces in Connectors
1.27 µm Ni underlay, 4 µm Sn-Bi
FFC mated with FPC flex cable, examined FPC, FFC, FFC-polyester side for whiskers without and with thermal shock at RT and HH.

Connector Interface	Range Wh. Length,µm	Ave. Wh. Length, µm	Max. Wh. Length, µm
FFC/No TS/ RT	0-105	42	105
FFC/TS/RT	0-27	14	27
FFC/No TS/HH	0-28	13	41
FFC/ TS/HH	0-30	9	30
FPC/No TS/RT	0-41	9	41
FPC/TS/RT	0	0	0
FPC/No TS/HH	0-17	3	17
FPC/TS/HH	0-20	4	20
FFC/No TS/RT/Poly	23-141	89	141
FFC/TS/RT/Poly	0-96	58	96
FFC/No TS/HH/Poly	0-41	16	41
FFC/TS/HH/Poly	16-77	33	77

The above table shows that the longest whiskers were observed on FFC terminals without TS at room temperature. This pronounced effect is explainable due to mechanical stress on the coating during the mating process. Reduced whisker response was found after thermal shock and heat and humidity. Possibly, some annealing action under heat relieves stress in the tin film and thus decreases whiskering. Large whiskers were also observed on FFC connector facing the polyester housings. Probably these long tin whiskers were generated due to excessive compressive stresses at the rigid interface.

4. Conclusions

6. The tin-bismuth process was evaluated critically with respect to temperature, agitation, current density, and additive concentration. The bath may be operated in a limited current density range (7.5-15 A/dm^2) with good current efficiencies. The deposits at 30 A/dm^2 were gray, had dendritic growth with rough appearance, and a significant decrease in current efficiencies.
7. The tin-bismuth process does not appear robust from a manufacturing viewpoint. Serious process issues such as immersion plating of bismuth, limited current density range, reduced current efficiencies, and control of the bismuth composition were observed.
8. Internal stress in deposits was minimal as found from flexure beam measurements. This was also evident from low total carbon values in deposits. Residual stresses by XRD were low and compressive in nature.
9. Whisker response under varying environmental conditions varied. Minimal whisker formation was observed under the harsh conditions of H&H.
10. Whisker growth appears to be application dependent. Resultant compressive forces at the mating interfaces play a pivotal role in whisker generation. Mechanical compressive stresses tend to be a dominant factor in dictating the overall whisker response. This was shown in the case of separable connectors where long whiskers were found.

Acknowledgements: The authors sincerely appreciate the technical suggestions from Steve Daly, and Steve Angeli of CDC Americas. We also thank FCI, Japan for providing tin-bismuth whisker data on FFC connectors. FIB work was done by courtesy of Dr. George Galyon, IBM.

References:

1. P. Elmgren,D. Dixon,R. Hilty,T. Moyer, S. Lal, A. Nitsche, & F. Teuber, " Pure Tin –The Finish of Choice for Connectors, " *IPC/JEDEC 4th International Conference on Lead Free Electronic Assemblies and Components*, Frankfurt, Germany, October 21-22, pp. 369-373, (2003).
2. P.L. Cavalotti, L.Nobili, G. Zangari & V. Sirtori, *SUR/FIN Conference, Session L*, pp 499-508 (1994).
3. Y.N. Sadana & T.K. Venkatachalam, *Met. Finish.* ,**80** (4), 61 (1981).
4. Isamu Yanada & Donald Gudeczauskas, *SUR/FIN* , pp 457-467 (1999).
5. G.G. Stoney," The Tension of Metallic Films Deposited by Electrolysis", *Proceedings of the Royal*

Society, A82, pp.72-175 (1909).

6. INEMI Test Method for Evaluating Tin Whisker Growth on Plated Surfaces, Revision 6.1, June 17,2004.
7. T.C. Frankin," Some mechanisms of Action of Additives in Electrodeposition Processes, " Surf. Coatings Technology, **30**, 415 (1987).
8. L. Oniciu & L. Munesan, "Some fundamental aspects of leveling & brightening in metal electrodeposition", J. Appl. Electrochem., **21**,565 (1991).
9. P. Harris, " The Growth of Tin Whiskers," ITRI Report #734, pp1-17, 1994
10. G.T. Galyon, " Annotated Tin Whisker Bibliography and Anthology", *INEMI Tin Whisker Modeling Project, version 1.2*, November 2003.
11. B. Z. Lee and D. N. Lee, " Spontaneous Growth Mechanism of Tin Whiskers", *Acta Metallurgica*, **46**(10), pp.3701-3714 (1998).
12. SAE-J784a, "Residual Stress Measurements by X-Ray Diffraction", Society of Automotive Engineers (SAE), 1971.
13. S. Lal and T. Moyer," Making the Lead-free Transition: The Enigma of Tin Whiskers in Connector Applications, " *AESF SUR/FIN Interfinish World Congress,* Chicago, June 4 , pp 234-253, (2004).
14. T. Moyer," Designed Experiment to determine the Reliability of Various Commercial Plating Baths and the Key Factors Affecting Whisker formation", Presented at 5th *IPC/JEDEC Lead-free Conference,Singapore,* August 2004.
15. S. Lal , and T. Moyer , " Role of Intrinsic Stresses in the Phenomena of Tin Whiskers in Electrical Connectors" Transactions on Electronic Packing Manufacturing, Vo. 28, No 1, January 2005. (in Print)
16. R.M. Fisher, L.S. Darken, and K.G. Carrol, " Accelerated Growth of Tin Whiskers," *Acta Metallurgica* , **2**, pp. 368-372 (1954).
17. G.T. Galyon, *Private Communication* (2004).

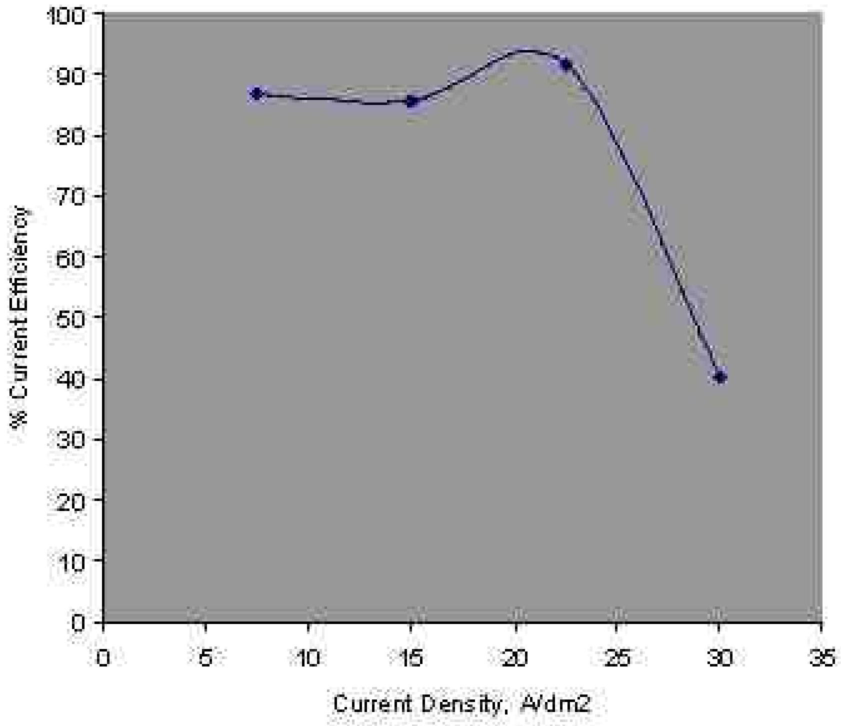

Figure 1: Current Density Vs. % Efficiency (Sn-Bi Bath @ 40ºC)

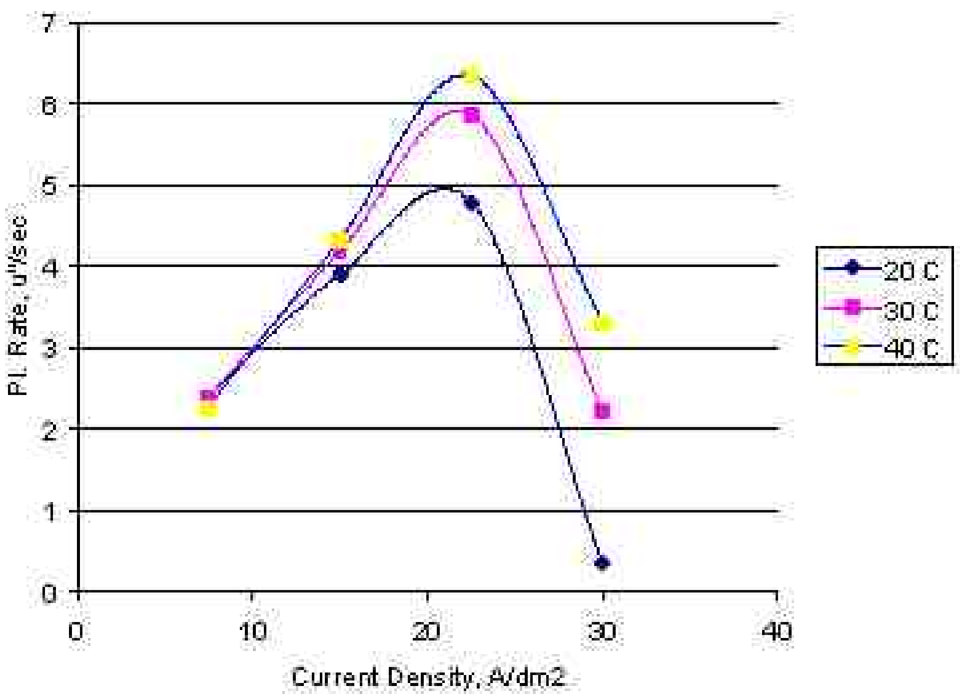

Figure 2: Current Density Vs. Pl. Rates (Sn-Bi) The effect of temperature on Plating rates

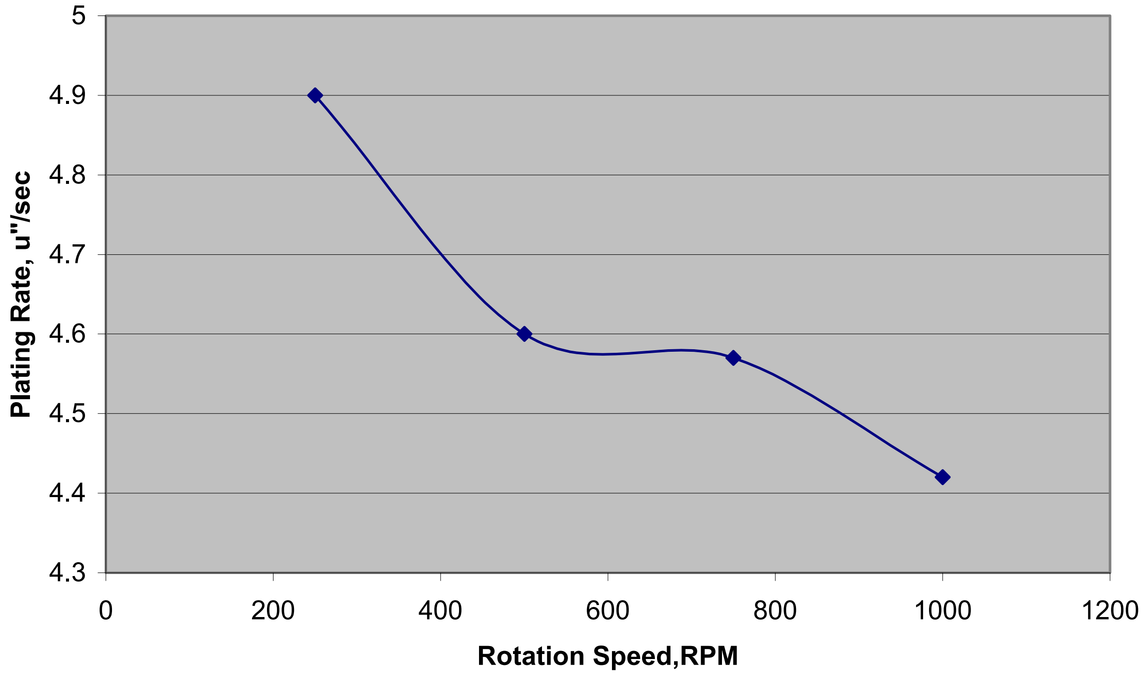

Figure 3: Agitation Effect (Tin-Bismuth Bath)

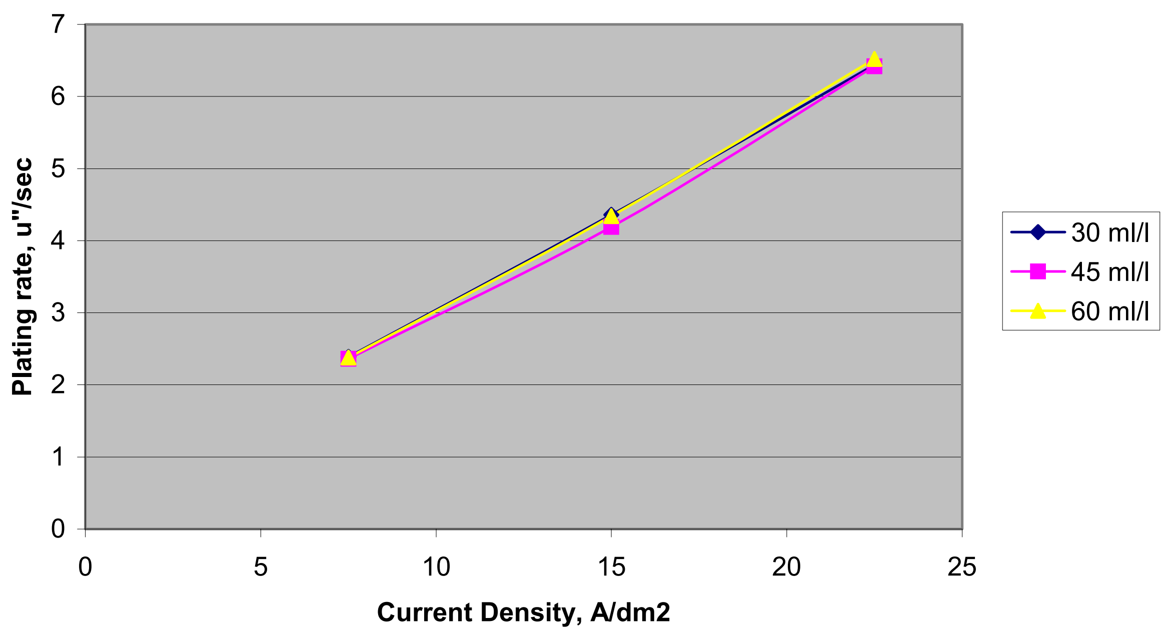

Figure 4: Current Density Vs. Plating Rate at varying Additive levels

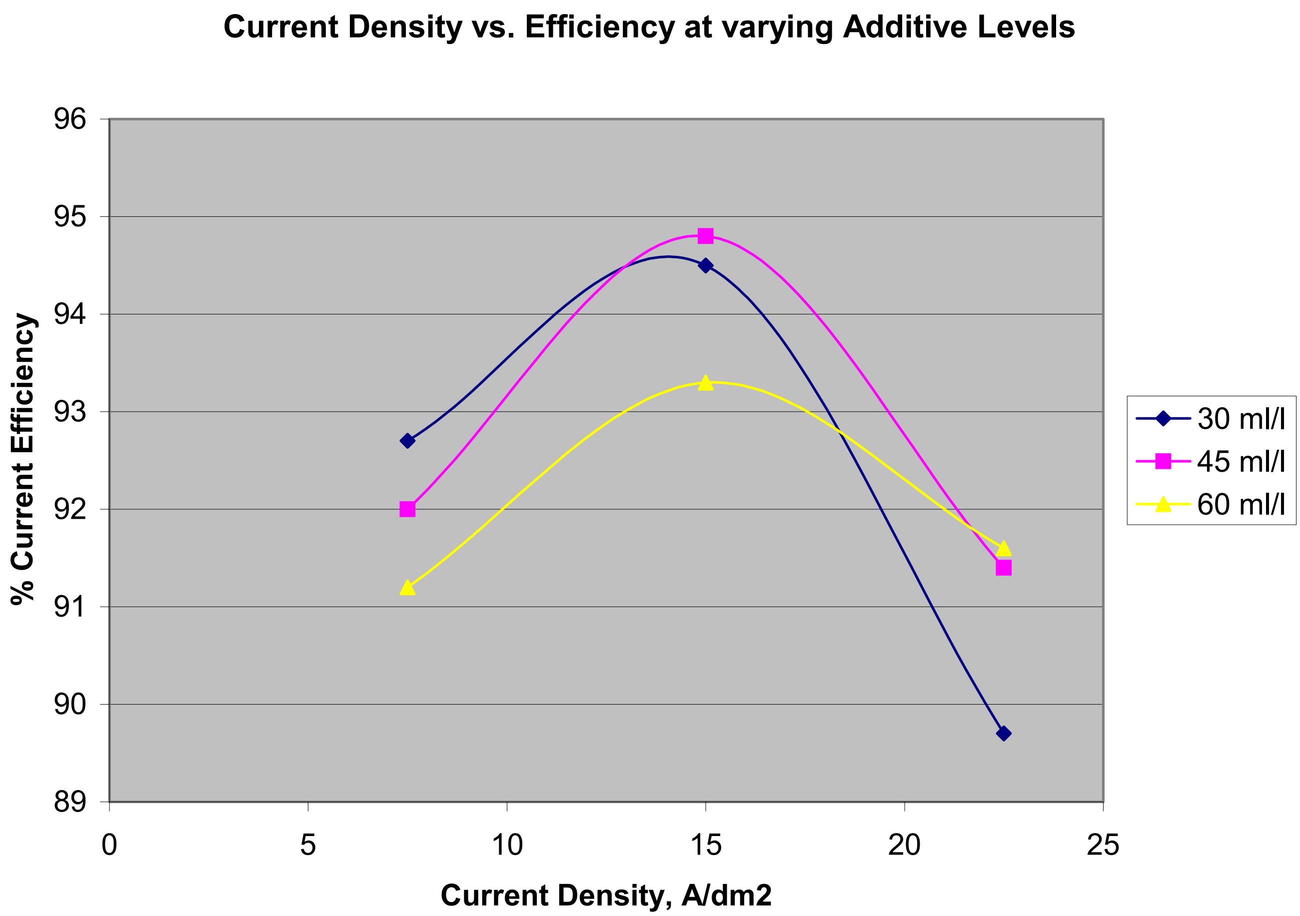

Figure 5: Current Density vs. Efficiency at varying Additive levels

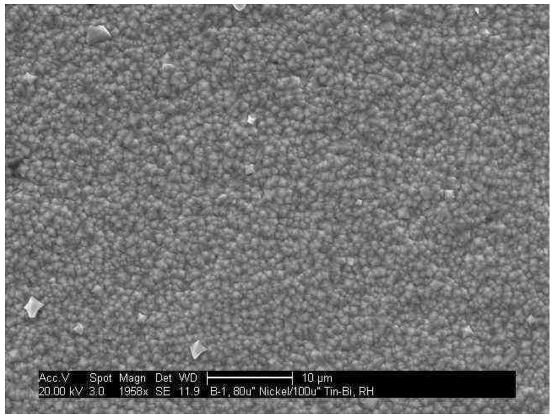

a) Morphology Sn-Bi (2.5 µm) over Nickel

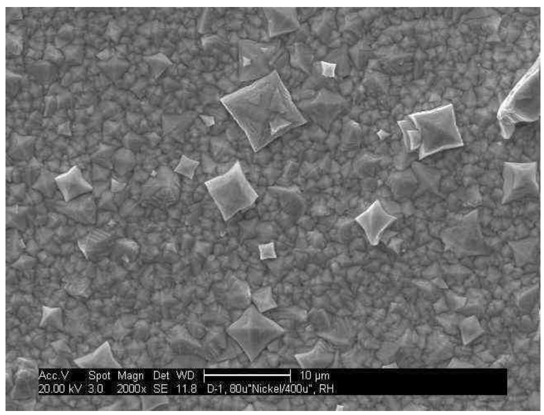

b) Morphology Sn-Bi (10 µm) over Nickel

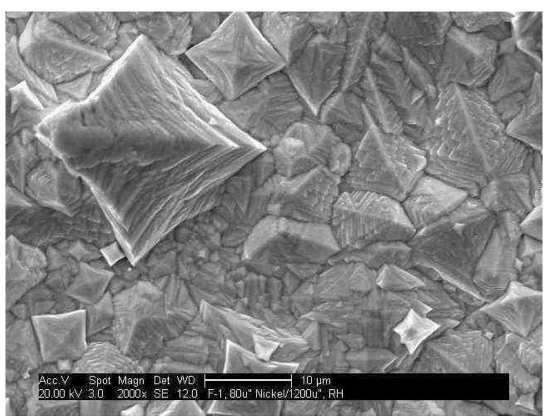

c) Morphology Sn-Bi (30 µm) over Nickel

Figure 6: SEM Morphology (2000X) of Tin-Bismuth Films at Current Densities a) 7.5 A/dm^2 b) 15 A/dm^2 c) 22.5 A/dm^2

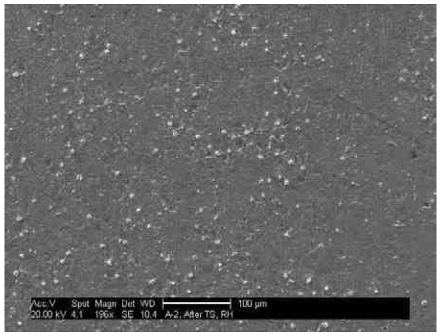

a) Sn-Bi (2.5 µm), no Ni after TS

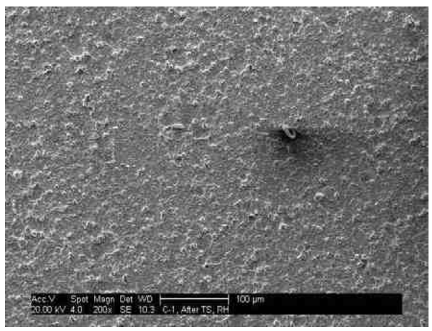

b) Sn-Bi (10 µm), no Ni after TS

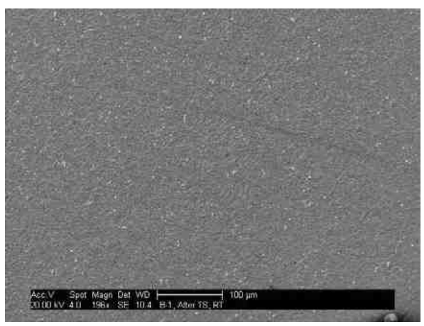

c) Sn-Bi (2.5 µm), 2 µm Ni after TS

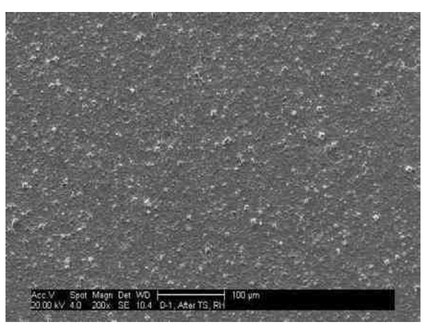

d) Sn-Bi (10 µm), 2 µm Ni after TS

Figure 7- a,b,c,d : OSEs response in Sn-Bi after 500 TS Cycles (SEM Photos 2000X)

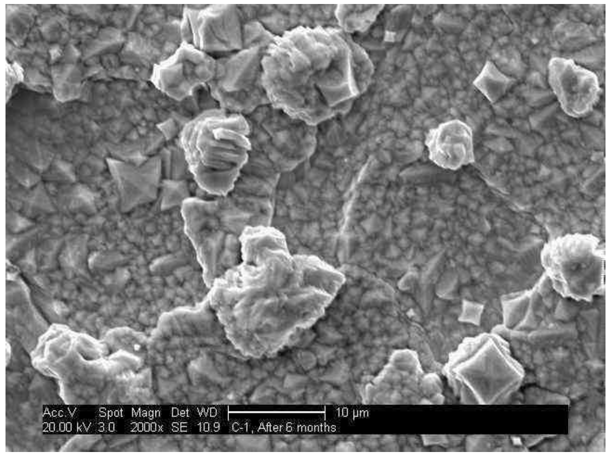

Figure 8: Sn-Bi (10 µm), 2 µm Ni after 6 month H&H

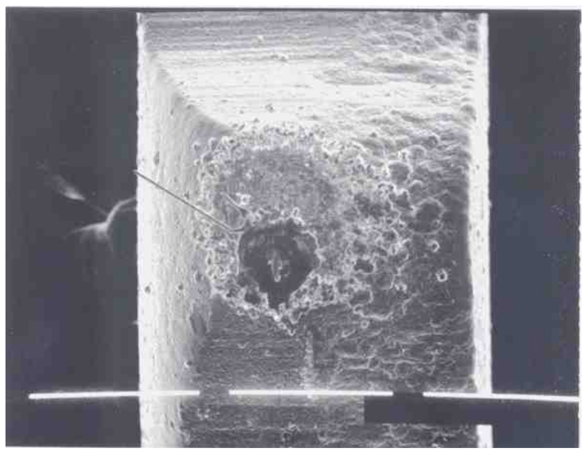

Figure 9: Tin Whisker 70 µm from Sn-Bi plating after mating

Figure 10: Tin whisker from tin-bismuth film under compressive force

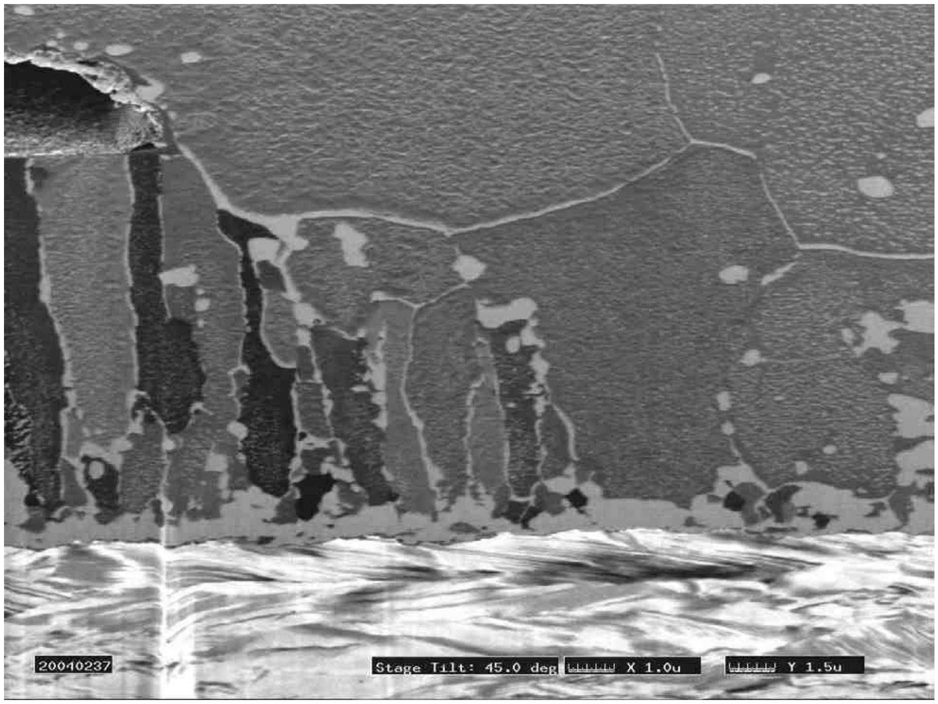

Figure 11: FIB Cross-section of Tin-copper film depicting IMC Formation

(Photo: Courtesy of Dr. George Galyon, IBM)